Electronic Supplementary Material (ESI) for Energy Advances.

Supporting Information

A Quick and Effective Strategy for the Synthesis of $Ti_3C_2T_x$ via Electrochemical Method

Shrabani De[a], Sourav Acharya[a], Satyanarayan Sahoo[b], and Ganesh Chandra Nayak*[a]

[a]Department of Chemistry, Indian Institute of Technology (ISM), Dhanbad-826004, Jharkhand, India

[b]P. G. Department of Chemistry, Berhampur University, Odisha, India, 760007

* E-mail Id of Corresponding authors: gcnayak@iitism.ac.in
Tel.: +91-326-2296563.

Experimental Section

1. Materials

All the chemicals used for the experiment are of analytical grade and utilized without further purification. MAX phase (Ti_3AlC_2, average particle size = 30 µm) was procured from Nanochemazone, India. Hydrogen fluoride (HF, 40%), and potassium hydroxide (KOH), polyvinyl alcohol (PVA, n=1750 ± 50) was procured from Avra, SRL, and TCI, India, respectively. N-methyl-2-pyrrolidone (NMP) was purchased from TCI, India. A DC power supply (UNI-T, UTP3315TFL, 0-30V, 0-5A) was used to provide a constant voltage across Pt electrodes during the electrochemical etching.

2. Characterization techniques

Characterization techniques used for the analysis of synthesized materials were X-ray powder diffraction (powder XRD, Rigaku, Smartlab with Cu Kα, wavelength 1.5406 Å, Bragg measurement, Smartlab studio II, D/teX Ultra-250 line detector), field-emission scanning electron microscopy (FESEM, Supra 55, Carl Zeiss, Germany, 5 kV, Signal A = InLens), Energy dispersive X-ray spectroscopy (EDS)-Mapping (Hitachi, S-3400N), Transmission electron microscope (TEM, Thermo Scientific, Talos F200X G2, 200 kV, Bright field), X-ray photoemission spectroscopy (XPS, PHI, 5000 versa probe III with Al

Kα, 10 kV, calibrated with adventitious C 1s at 284.8 eV, peakfit software, Gauss Amp, Bg=linear, other fitting parameters are summarized in Table S4), Micro-Raman spectroscopy (HORIBA Scientific, France LabRAM HR-UV-Open, Laser excitation wavelength 532 nm), and electrochemical workstation (Metrohm Autolab M204).

3. Synthesis of electrochemically etched MXene (EMX)

In a plastic beaker, 500 mg of Ti_3AlC_2 was added in 10 ml HF solution. Two platinum strips were dipped into the solution and connected with a power supply. The solution mixture was kept under stirring at an applied voltage of 0.6 V at room temperature for 2 h. After that, the solution was neutralized with distilled water until pH = 6 and centrifuged to separate the sample. Then, the sample was dried at 60 °C for 12 h to obtain $Ti_3C_2T_x$ (EMX).

4. Synthesis of $(Et_3HN)^+(NO_3)^-$

Typically, concentrated HNO_3 was added drop-wise into 15 ml of triethylamine solution until the solution become almost neutral.[1] Then, the obtained viscous ionic liquid is stored in vacuum.

5. Synthesis of delaminated-EMX (d-EMX)

The synthesized EMX was delaminated using ionic liquid $[(Et_3HN)^+(NO_3)^-]$. Briefly, 300 mg EMX was added into 20 ml of ionic liquid. Argon gas was purged into the solution to remove the dissolved oxygen gas and kept in a sealed bottle. Then, the mixture was shaken in orbital shaker at 120 rpm, for 6 h at 10 °C. After that, the sample was separated by centrifugation and washing with water and ethanol. Finally, the product was dried at 60 °C for 12 h to obtain d-EMX.

5. Synthesis of PVA-KOH gel electrolyte

The PVA-KOH gel electrolyte was prepared following the common conventional method.[2] Typically, 20 ml 9 wt% PVA solution was first prepared at 90 °C. Then, 10 wt% KOH solution (10 ml) was added drop-wise into the PVA solution. The obtained semi-transparent liquid was used as gel electrolyte.

6. Electrochemical study for supercapacitor

The electrochemical performance in two-electrode configuration was analyzed in PVA-KOH gel electrolyte. Carbon fibre mat was used as current collector and electroactive material was brushed over to prepare positive and negative electrode. The electroactive material slurry was prepared by mixing the prepared sample (80 wt%), carbon black (15 wt%), and PVDF (5 wt%) with few drops of NMP). Cyclic voltammetry (CV) and the galvanostatic charging–discharging (GCD) study were carried out to evaluate the electroactivity of the prepared d-EMX as anode. The mass loading of active material was 10 mg. The electrochemical impedance spectroscopy (EIS) analysis was conducted from a frequency of 1 MHz to 1 Hz at 10 mV amplitude at room temperature. The specific capacitance (F g^{-1}) was evaluated using GCD plots by using the equation:[3]

Specific capacitance = $\frac{2 \times i \times \Delta t}{m \times \Delta V}$ (Equation S1)

Where i is the charging–discharging current, Δt is the time required in seconds for the discharge cycle, m is the mass loaded, and ΔV is the voltage range.

The specific energy density (W h kg^{-1}) and power density (W kg^{-1}) were evaluated using the following equations:[4]

Energy density = $\frac{C \Delta V^2}{7.2}$ (Equation S2)

Power density = $\frac{E \times 3600}{\Delta t}$ (Equation S3)

7. Electrocatalytic performance study

The electrocatalytic studies performed using d-EMX-modified glassy carbon electrodes (GCE). The GCE was of 3 mm diameter. The electrode was cleaned with alumina slurry for 2 minutes, and then washed with water for several times and dried in oven. The GCE was coated by drop casting of the d-EMX ink, prepared using above mentioned method. The as prepared electrode was used as working electrode, a Pt strip was used a counter electrode while the reference electrode taken was a Ag/AgCl electrode.

The potentials of the electrode materials were determined taking reversible hydrogen electrode (RHE) as the reference. The equation of the electrode potential with respect to RHE is given by:

$E_{RHE} = E^{\circ}_{Ag/AgCl} + 0.059 \times pH + E_{Ag/AgCl}$ (Equation S4)

where, $E^{\circ}_{Ag/AgCl}$ (0.197 V) is the standard reduction potential of Ag/AgCl electrode at 25°C and $E_{Ag/AgCl}$ is the electrode potential of the nanomaterial-coated-GCE with reference to Ag/AgCl. The coated and exposed geometrical surface area of each of the electrodes was calculated to be 0.071 cm^2. Since, 1 M KOH (pH=14) solution was used as a supporting electrolyte for study of OER,

therefore, $E_{RHE} = (1.023 + E_{Ag/AgCl})\, V$ (Equation S5)

On the other hand, 1 M H_2SO_4 (pH=0) solution was used as a supporting electrolyte for study of HER,

therefore, $E_{RHE} = (0.197 + E_{Ag/AgCl})\ V$ (Equation S6)

The overpotential (η) is calculated by subtracting the water splitting potential (1.23 V) from the working electrode potential, i.e.,

$\eta = (E_{RHE}$ - 1.23$)\ V$ (Equation S7)

Table S1. Comparison of previously reported electrochemical etching methods with this study.

MXene	Etchant	Etching time	Voltage (V)	Temperature (°C)	Ref.
Ti_2CT_x, Cr_2CT_x, V_2CT_x	2 M HCl	9 h	0.7-1.0	50	[5]
Ti_2CT_x	2 M HCl	5 days	0.6	RT	[6]
$Ti_3C_2T_x$	1 M NH_4Cl + 0.2 M TMA-OH	5 h	5	RT	[7]
$Ti_3C_2T_x$	HF (40 %)	2 h	0.6	RT	This work

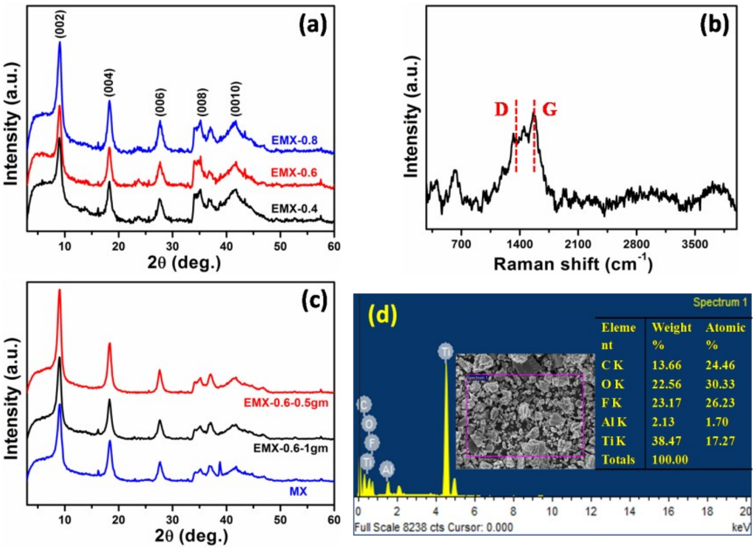

Element	Weight %	Atomic %
C K	13.66	24.46
O K	22.56	30.33
F K	23.17	26.23
Al K	2.13	1.70
Ti K	38.47	17.27
Totals	100.00	

Fig. S1 (a) XRD of EMX synthesized at different applied voltages performed for 120 minutes, (b) Raman spectrum of EMX-0.6-120 min, (c) XRD comparison of EMX-0.6-120 min samples prepared in large batches and chemically etched MXene (MX) prepared under same condition without the applied voltage, (d) EDS analysis of EMX-0.6-120 min.

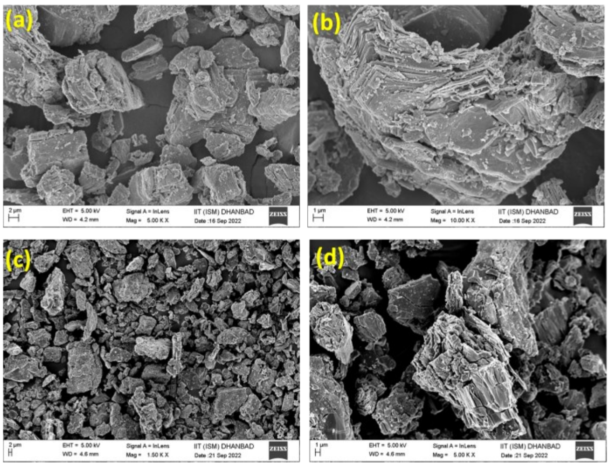

Fig. S2 FESEM images of (a, b) EMX-0.6 10 min, and (c, d) EMX-0.6-20 min.

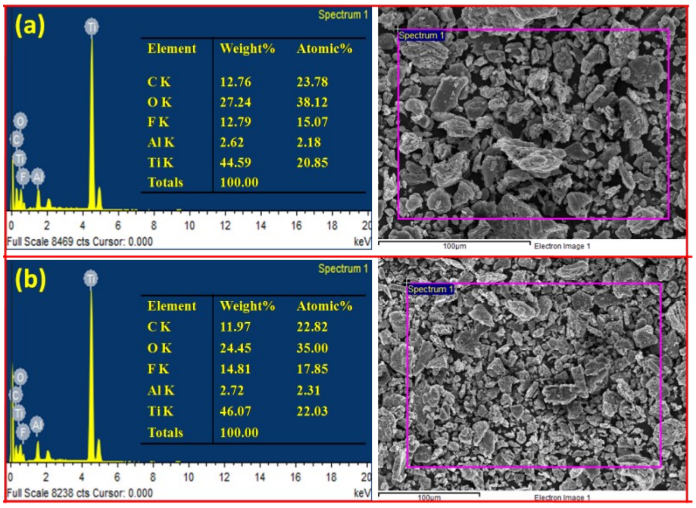

(a)

Element	Weight%	Atomic%
C K	12.76	23.78
O K	27.24	38.12
F K	12.79	15.07
Al K	2.62	2.18
Ti K	44.59	20.85
Totals	100.00	

(b)

Element	Weight%	Atomic%
C K	11.97	22.82
O K	24.45	35.00
F K	14.81	17.85
Al K	2.72	2.31
Ti K	46.07	22.03
Totals	100.00	

Fig. S3 EDS analysis of (a) EMX-0.6 10 min, and (b) EMX-0.6-20 min.

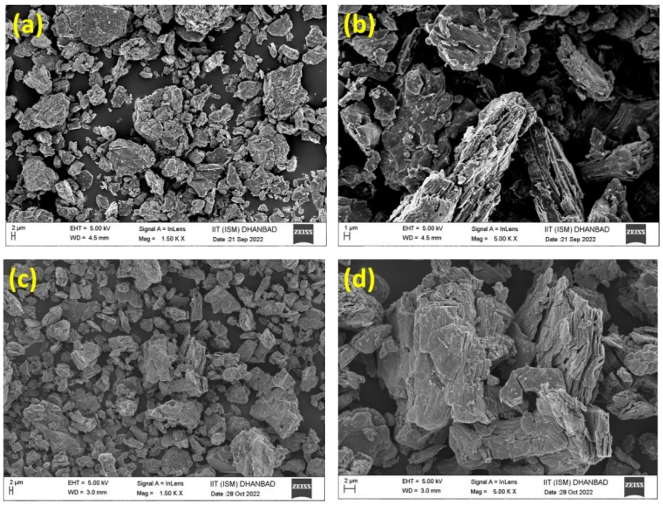

Fig. S4 FESEM images of (a, b) EMX-0.6 40 min, and (c, d) EMX-0.6-60 min.

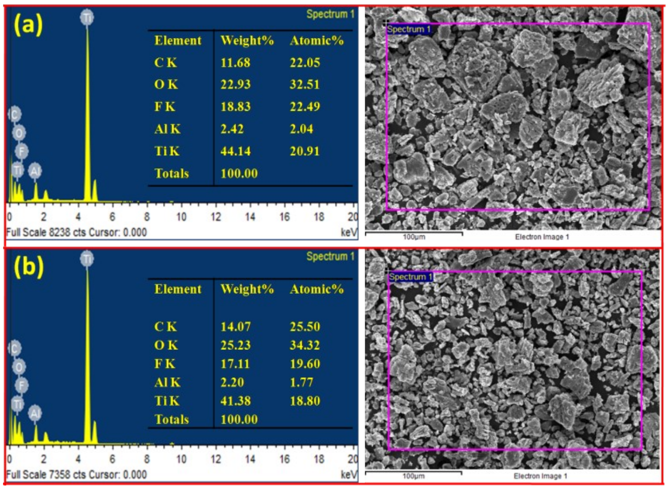

(a)

Element	Weight%	Atomic%
C K	11.68	22.05
O K	22.93	32.51
F K	18.83	22.49
Al K	2.42	2.04
Ti K	44.14	20.91
Totals	100.00	

(b)

Element	Weight%	Atomic%
C K	14.07	25.50
O K	25.23	34.32
F K	17.11	19.60
Al K	2.20	1.77
Ti K	41.38	18.80
Totals	100.00	

Fig. S5 EDS analysis of (a) EMX-0.6 40 min, and (b) EMX-0.6-60 min.

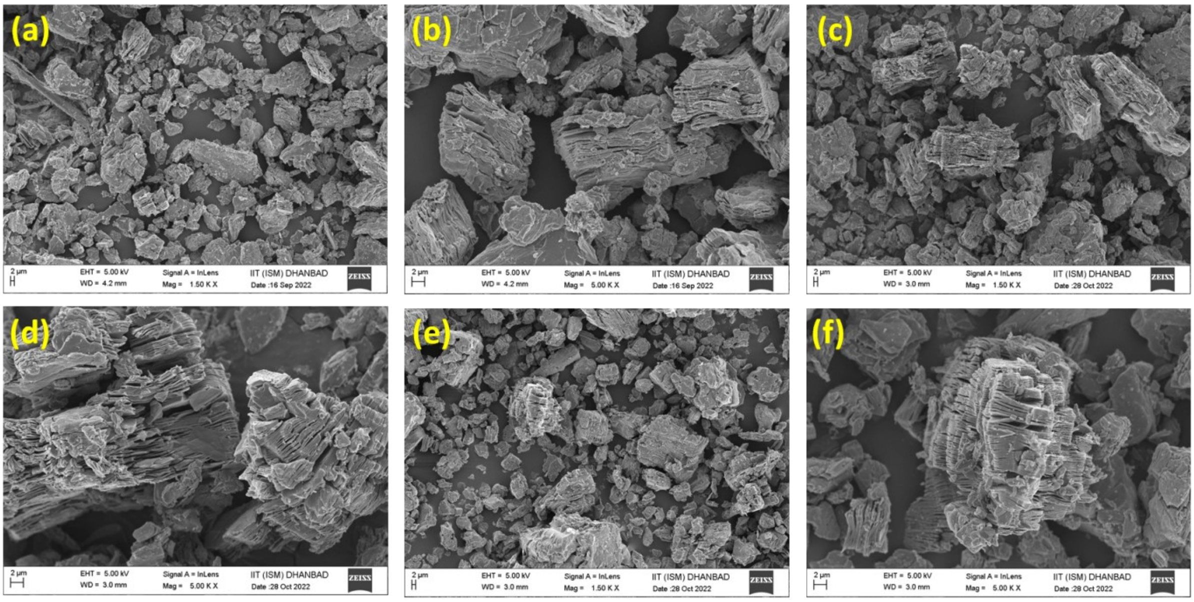

Fig. S6 FESEM images of (a, b) EMX-0.6 80 min, (c, d) EMX-0.6-100 min, and (e, f) EMX-0.6-120 min.

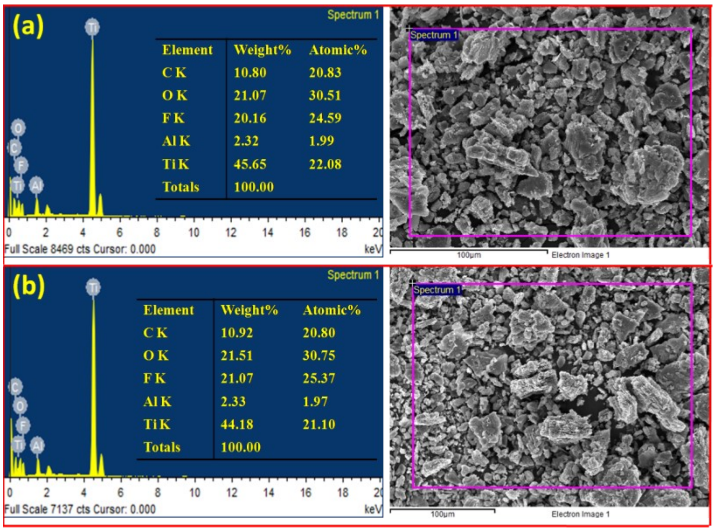

(a)

Element	Weight%	Atomic%
C K	10.80	20.83
O K	21.07	30.51
F K	20.16	24.59
Al K	2.32	1.99
Ti K	45.65	22.08
Totals	100.00	

(b)

Element	Weight%	Atomic%
C K	10.92	20.80
O K	21.51	30.75
F K	21.07	25.37
Al K	2.33	1.97
Ti K	44.18	21.10
Totals	100.00	

Fig. S7 EDS analysis of (a) EMX-0.6 80 min, and (b) EMX-0.6-100 min.

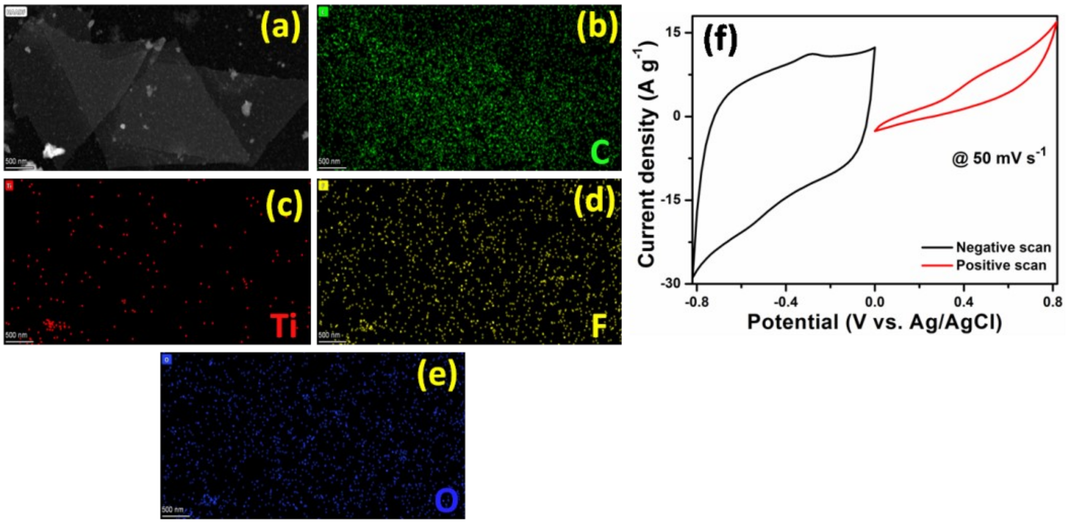

Fig. S8 (a) TEM mapping area, and (b-e) elemental mapping of C, Ti, F, and O, respectively of d-EMX, (f) electrochemical performance of d-EMX in positive and negative potential window in 1 M KOH electrolyte in three electrode system.

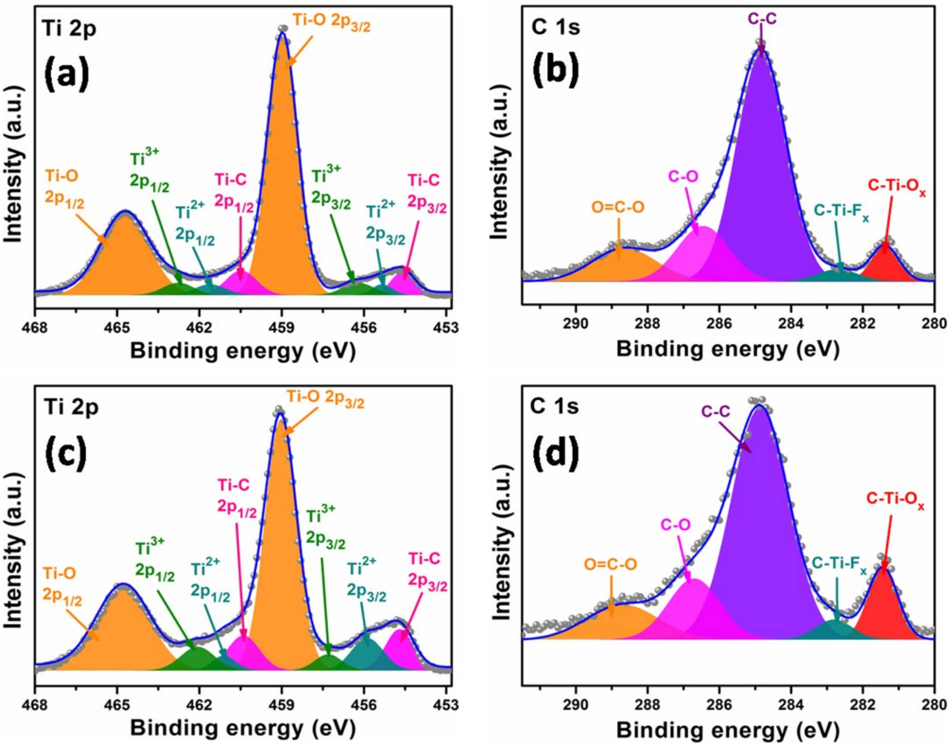

Fig. S9 Deconvoluted XPS spectra of (a) Ti 2p, and (b) C 1s of EMX-0.6-60 min and (c) Ti 2p, and (d) C 1s of EMX-0.6-100 min.

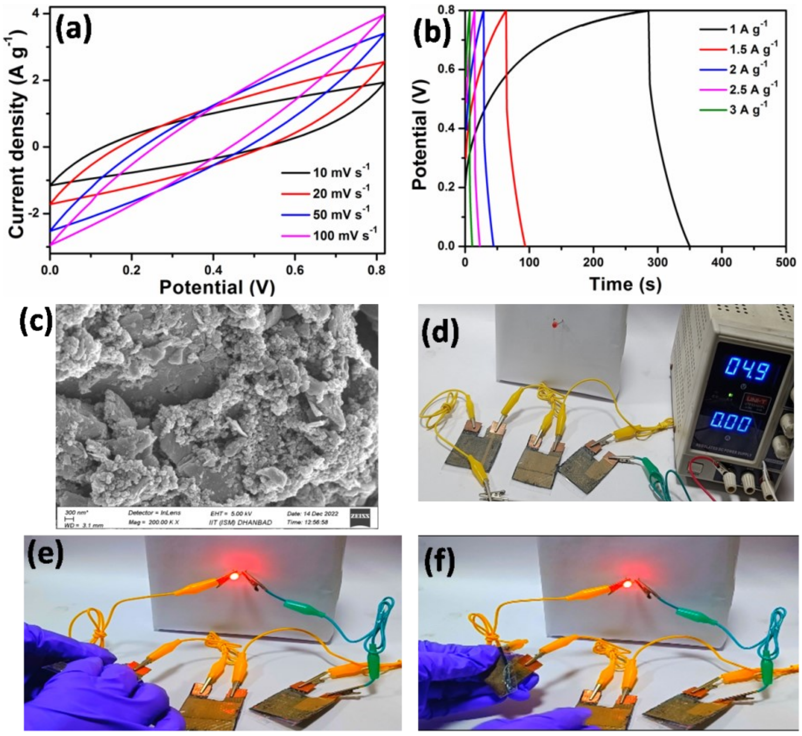

Fig. S10 (a) CV curves at different scan rates, and (b) GCD profiles at different current densities of ASSASC device, (c) FESEM image of the anode material (d-EMX+carbon black+PVDF) after cyclic stability study, (d) charging set up, and (e, f) flexibility of the devices connected in series.

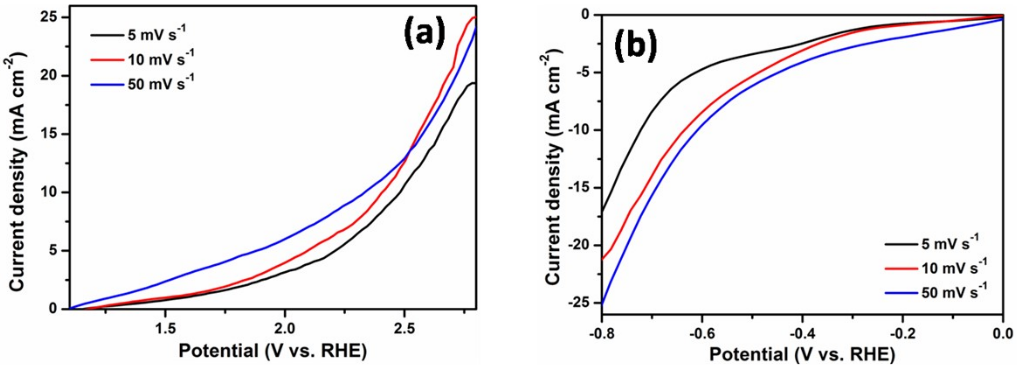

Fig. S11 Electrocatalytic performance of d-EMX (a) LSV profile at different scan rates in 1 M KOH for OER, and (b) LSV profile at different rates in 1 M H_2SO_4 for HER.

Table S2: Comparative study of electrochemical performance of d-EMX with some priorly investigated $Ti_3C_2T_x$-based devices.

$Ti_3C_2T_x$-based devices (+)//(-)	**Electrolyte**	**Potential range (V)**	**Specific capacitance (F g^{-1})**	**Current density**	**Energy density (Wh kg^{-1})**	**Power density (W kg^{-1})**	**Retention of specific capacitance**	**Number of cycles**	**Ref.**

							(%)		
$Ti_3C_2T_x$/NCF//$Ti_3C_2T_x$/NCF	PVA/KOH	1.0	63	1 A g^{-1}	8.75	1871	96	2500	[8]
$NiCo_2O_4$@rGO/ACF// $Ti_3C_2T_x$/ACF	PVA/KOH	1.5	141.9	5 mA cm^{-2}	44.36	985	90.48	4500	[9]
$Ti_3C_2T_x$/MPF//$Ti_3C_2T_x$/MPF	PVA/H_2SO_4	0.6	40.7	0.01 A g^{-1}	-	-	95.9	7000	[10]
Ti_3C_2/CuS//Ti_3C_2	1 M KOH	1.5	49.3	1 A g^{-1}	15.4	750.2	82.4	5000	[11]
rGO//$Ti_3C_2T_x$	1 M H_2SO_4	1.1	48	2 mV s^{-1}	8	50	76	1000	[12]
$Ti_3C_2T_x$/CF//$Ti_3C_2T_x$/CF	PVA/KOH	1.0	76	0.5 A g^{-1}	10.6	125.5	99.8	5000	[13]
$Ti_3C_2T_x$//AC	PVA-Li_2SO_4	1.0	46	25 mV s^{-1}	5.5	500	98	3000	[14]
Phen@rGO// $Ti_3C_2T_x$	3 M H_2SO_4	1.4	64	5 mV s^{-1}	17.4	~250	80	30000	[15]
C3@rGO//$Ti_3C_2T_x$	3 M H_2SO_4	1.5	64	10 mV s^{-1}	20	480	80	10000	[16]
d-Ti_3C_2/NF//d-Ti_3C_2	6 M KOH	1.6	51.1	0.5 A g^{-1}	18.1	397.8	80.6	5000	[17]
MnO_2//d-EMX	**PVA/KOH**	**0.8**	**162**	**1 A g^{-1}**	**14.4**	**800**	**83.6**	**10000**	**This work**

NCF-N-doped carbon foam; ACF-acid treated carbon fibre; MPF-2D metal porphyrin framework; CF-biomass derived carbon fibre; AC-activated carbon; rGO-reduced graphene oxide; Phen – Phenothiazine; d-Ti_3C_2-delaminated Ti_3C_2 ; NF-nickel foam.

Table S3. Comparison of electrocatalytic activity with some previously reported MXene based materials.

Electrocatalyst	Application	Electrolyte	Onset potential (V)	Ref.
Ni/Fe doped GO@MXene	OER	1 M KOH	1.5	[18]
NiCoS/$Ti_3C_2T_x$	OER	1 M KOH	1.53	[19]
$Ti_3C_2T_x$	HER	0.1 M H_2SO_4	-0.25	[20]
Ti_2CT_x	HER	0.5 M H_2SO_4	-0.22	[21]
d-EMX	**OER**	**1 M KOH**	**1.45**	**This work**
d-EMX	**HER**	**1 M H_2SO_4**	**-0.19**	**This work**

References

1. C. K. Maity, D. K. Santra, K. Verma, S. Sahoo, S. Cotts, D. Akinwande, V. Berry and G. C. Nayak, *Composites Part B: Engineering*, 2021, **212**, 108728.
2. H. Ur-Rehman, A. Shuja, M. Ali, M. S. Khan, I. Murtaza and H. Meng, *Journal of Materials Science: Materials in Electronics*, 2022, **33**, 2322-2335.
3. S. De, C. K. Maity, S. Sahoo and G. C. Nayak, *ACS Applied Energy Materials*, 2021, **4**, 3712-3723.
4. M. Chuai, K. Zhang, X. Chen, Y. Tong, H. Zhang and M. Zhang, *Chemical Engineering Journal*, 2020, **381**, 122682.
5. S.-Y. Pang, Y.-T. Wong, S. Yuan, Y. Liu, M.-K. Tsang, Z. Yang, H. Huang, W.-T. Wong and J. Hao, *Journal of the American Chemical Society*, 2019, **141**, 9610-9616.
6. W. Sun, S. Shah, Y. Chen, Z. Tan, H. Gao, T. Habib, M. Radovic and M. Green, *Journal of Materials Chemistry A*, 2017, **5**, 21663-21668.
7. S. Yang, P. Zhang, F. Wang, A. G. Ricciardulli, M. R. Lohe, P. W. Blom and X. Feng, *Angewandte Chemie*, 2018, **130**, 15717-15721.
8. L. Sun, G. Song, Y. Sun, Q. Fu and C. Pan, *ACS Applied Materials & Interfaces*, 2020, **12**, 44777-44788.
9. A. M. Patil, N. Kitiphatpiboon, X. An, X. Hao, S. Li, X. Hao, A. Abudula and G. Guan, *ACS Applied Materials & Interfaces*, 2020, **12**, 52749-52762.
10. W. Zhao, J. Peng, W. Wang, B. Jin, T. Chen, S. Liu, Q. Zhao and W. Huang, *Small*, 2019, **15**, 1901351.
11. Z. Pan, F. Cao, X. Hu and X. Ji, *Journal of Materials Chemistry A*, 2019, **7**, 8984-8992.
12. A. M. Navarro-Suárez, K. L. Van Aken, T. Mathis, T. Makaryan, J. Yan, J. Carretero-González, T. Rojo and Y. Gogotsi, *Electrochimica Acta*, 2018, **259**, 752-761.
13. L. Sun, Q. Fu and C. Pan, *Journal of Hazardous Materials*, 2021, **410**, 124565.
14. T.-H. Chang, T. Zhang, H. Yang, K. Li, Y. Tian, J. Y. Lee and P.-Y. Chen, *Acs Nano*, 2018, **12**, 8048-8059.
15. M. Boota, M. Bécuwe and Y. Gogotsi, *ACS Applied Energy Materials*, 2020, **3**, 3144-3149.
16. M. Boota, M. Rajesh and M. Bécuwe, *Materials Today Energy*, 2020, **18**, 100532.
17. J. Guo, Y. Zhao and T. Ma, *Electrochimica Acta*, 2019, **305**, 164-174.
18. S. K. Raj, G. R. Bhadu, P. Upadhyay and V. Kulshrestha, *International Journal of Hydrogen Energy*, 2022, **47**, 41772-41782.

19. H. Zou, B. He, P. Kuang, J. Yu and K. Fan, *ACS applied materials & interfaces*, 2018, **10**, 22311-22319.
20. J. Filip, S. Zavahir, L. Lorencova, T. Bertok, A. B. Yousaf, K. A. Mahmoud, J. Tkac and P. Kasak, *Journal of The Electrochemical Society*, 2019, **166**, H54.
21. Z. W. Seh, K. D. Fredrickson, B. Anasori, J. Kibsgaard, A. L. Strickler, M. R. Lukatskaya, Y. Gogotsi, T. F. Jaramillo and A. Vojvodic, *ACS Energy Letters*, 2016, **1**, 589-594.